Elastic Scattering of 30.3-MeV Polarized Protons from ^{40}Ca, ^{56}Fe, and ^{59}Co†

V. Hnizdo, O. Karban, and J. Lowe
Department of Physics, University of Birmingham, Birmingham, England

and

G. W. Greenlees and W. Makofske
Department of Physics, University of Minnesota, Minneapolis, Minnesota 55455

(Received 17 December 1970)

Results are presented for the elastic scattering of 30.3-MeV polarized protons from targets of ^{40}Ca, ^{56}Fe, and ^{59}Co. The angular region from 20 to 165° is covered with an absolute accuracy in the polarization measurements of about 0.01. The data, together with corresponding differential-cross-section data reported elsewhere, are analyzed using the optical model in a manner similar to that used for corresponding data for ^{58}Ni, ^{120}Sn, and ^{208}Pb. The present results confirm the trends with mass number found earlier, suggesting that present forms of the model are only satisfactory for large nuclei (^{208}Pb), and that for lighter systems modifications are needed.

I. INTRODUCTION

A recent analysis[1] of accurate differential-cross-section and polarization data for ^{58}Ni, ^{120}Sn, and ^{208}Pb at 30.3 MeV was carried out using both the standard 10-parameter optical model[2] and the folding version of Greenlees, Pyle, and Tang[3,4] (GPT) in which the real parts of the optical-model potential (central, isospin, and spin-orbit) are expressed in terms of nuclear-density distributions and components of the two-body force. In the standard optical-model analysis, it was found that the fits to the data improved with increase in mass number of the target nucleus. For the heaviest element (^{208}Pb), the parameters obtained in fitting either cross-section data, polarization data, or both, were almost identical indicating that a good model representation was being obtained irrespective of the type of data used. However, for ^{58}Ni and ^{120}Sn, significant differences were found which were attributed to shortcomings of the model description. It was further noted that the spin-orbit radius parameters found for ^{58}Ni and ^{120}Sn (~1.0 F) using the standard model were appreciably lower than for ^{208}Pb (1.15 F) contrary to expectations based on physical arguments.

The folding-model analysis likewise showed an improvement in χ^2 values with increasing target mass number. However, for ^{120}Sn, and more so for ^{58}Ni, the representation of the data was found to be less satisfactory with the folding model than the standard version, with χ^2 values being 2 to 4 times greater and the visual quality of the fits noticeably worsened. This was attributed to the coupling of the real central and spin-orbit geometries inherent in the folding model. The improvement in the fits obtained with the standard model for lighter elements which led to a peaking of the spin-orbit term about 0.5 F inside the nucleon half-density point and in a region of nearly constant density is difficult to understand physically.

Further, analyses of inelastic data for medium-weight nuclei showed that improved fits are obtained when the folding model is used to describe the interaction,[5] or when the standard model[6] is used with equal real and spin-orbit radii. These results, together with the absence of an isospin dependence of the real-central-potential volume integrals, suggested that an optical-model description of the type normally used for elastic scattering data is more applicable to heavy nuclei, and that for smaller systems some second-order processes are playing a nonnegligible role.

The present work presents additional accurate polarization data for medium-A nuclei at 30.3 MeV, thereby allowing a test of the conclusions of Ref. 1. The angular range from 20 to 165° was studied for ^{40}Ca, ^{56}Fe, and ^{59}Co; the absolute polarization error in general was less than 0.01 at forward angles and did not exceed 0.02 at angles greater than 130°. Both cross-section and polarization data of a similar quality to that used in Ref. 1 are analyzed with the 10-parameter standard optical model and the folding version of GPT. The results of this analysis are compared with those of Ref. 1.

II. EXPERIMENT AND RESULTS

The experiment was performed using the polarized-source facility of the Rutherford Laboratory proton linear accelerator. The arrangement was the same as that described in Ref. 1, except that strip targets were not used. The over-all angular resolution was ±1.7° for $\theta \geq 60°$ and ±1.5° for $\theta < 60°$.

TABLE I. Polarization results for 30.3-MeV protons elastically scattered by ^{40}Ca, ^{56}Fe, and ^{59}Co. The overall angular resolution was ±1.7° for $\theta \geq 60°$ and ±1.5° for $\theta < 60°$.

Angle (lab) (deg)	$P(\theta)$ ^{40}Ca	$P(\theta)$ ^{56}Fe	$P(\theta)$ ^{59}Co
20	−0.186 ± 0.004	−0.182 ± 0.005	−0.193 ± 0.003
22.5	−0.273 ± 0.002	−0.217 ± 0.003	•••
25	−0.375 ± 0.004	−0.394 ± 0.006	−0.345 ± 0.004
27.5	•••	•••	−0.094 ± 0.008
30	−0.652 ± 0.004	0.646 ± 0.014	0.651 ± 0.010
32.5	−0.282 ± 0.007	0.507 ± 0.006	0.429 ± 0.005
35	0.187 ± 0.004	0.274 ± 0.005	0.230 ± 0.004
37.5	0.224 ± 0.004	•••	0.110 ± 0.003
40	0.156 ± 0.003	0.043 ± 0.006	−0.001 ± 0.001
45	0.011 ± 0.002	−0.142 ± 0.003	−0.177 ± 0.004
47.5	−0.054 ± 0.002	•••	•••
50	−0.129 ± 0.003	−0.349 ± 0.008	−0.417 ± 0.005
55	−0.244 ± 0.004	−0.513 ± 0.004	−0.483 ± 0.006
60	−0.320 ± 0.003	0.165 ± 0.009	0.389 ± 0.003
65	−0.066 ± 0.005	0.636 ± 0.006	0.565 ± 0.004
70	0.548 ± 0.003	0.451 ± 0.007	0.360 ± 0.004
75	0.650 ± 0.005	0.231 ± 0.007	0.152 ± 0.004
80	0.491 ± 0.004	0.015 ± 0.009	−0.060 ± 0.006
85	0.351 ± 0.005	−0.152 ± 0.010	−0.138 ± 0.006
90	0.175 ± 0.003	0.015 ± 0.009	0.140 ± 0.005
95	0.037 ± 0.003	0.601 ± 0.011	0.659 ± 0.004
100	0.060 ± 0.005	0.919 ± 0.011	0.894 ± 0.005
105	0.374 ± 0.004	0.877 ± 0.010	0.818 ± 0.004
110	0.773 ± 0.005	0.755 ± 0.016	0.627 ± 0.005
115	0.934 ± 0.004	0.507 ± 0.015	0.437 ± 0.006
120	0.989 ± 0.005	0.379 ± 0.015	0.280 ± 0.007
125	0.976 ± 0.004	0.181 ± 0.018	0.199 ± 0.008
130	0.897 ± 0.006	0.143 ± 0.028	0.360 ± 0.013
135	0.593 ± 0.019	0.460 ± 0.040	0.598 ± 0.019
140	0.266 ± 0.010	0.870 ± 0.038	0.861 ± 0.013
145	0.335 ± 0.016	0.962 ± 0.030	0.975 ± 0.015
150	0.326 ± 0.007	0.990 ± 0.016	0.894 ± 0.010
155	0.267 ± 0.012	0.869 ± 0.029	0.700 ± 0.015
160	0.128 ± 0.010	0.633 ± 0.017	0.406 ± 0.011
165	−0.035 ± 0.012	0.210 ± 0.035	0.038 ± 0.021

The angular accuracy was ±0.25° in all cases. The target thicknesses were 200 keV for all three targets, and enabled the first inelastic group to be resolved from the elastic at all angles. The energy was maintained within ±100 keV of that used in obtaining the corresponding differential-cross-section data of Ridley and Turner[7] (30.3 MeV). The present results together with errors are listed in Table I.

III. ANALYSIS AND DISCUSSION

The present polarization data, along with the corresponding differential-cross-section data,[7] have been analyzed using two versions of the optical model: (1) the standard version in which all the terms of the potential are parametrized independently, and (2) the folding model of Greenlees, Pyle, and Tang[3,4] in which the real parts of the potential are derived from the nuclear nucleon distributions via the two-body force.

The differential-cross-section data of Ridley and Turner consist of approximately 80 points per element covering the angular range 4–162° in 2° steps. The present polarization data consist of approximately 40 points per element covering an angular range 20 to 165° in 2.5 and 5° steps. In order to remain consistent with Ref. 1, only every other differential-cross-section point was used. Reaction-cross-section data at 28.5 MeV were also available[8] for the elements studied here. These data were not included explicitly in the analysis but the predictions obtained in all cases were always consistent with the errors in the experimental data.

A modified version of the computer code RAROMP[9] (which included both standard and folding versions of the model) was used in these studies together with the University of Minnesota CDC-6600 computer. The program averaged the polarization angular distributions over the experimental angular acceptances, and varied the model parameters to determine a χ^2 minimum.

A. Standard Optical-Model Analysis

The potential used had the form

$$V(r) = -V_{RS} f(r, r_R, a_R) - iW_V f(r, r_I, a_I) + i4a_I W_S \frac{d}{dr} f(r, r_I, a_I) + \left(\frac{\hbar}{m_\pi c}\right)^2 V_{so} \frac{1}{r} \frac{d}{dr} f(r, r_{so}, a_{so}) \vec{\sigma} \cdot \vec{I} + V_C(r), \quad (1)$$

where

$$f(r, r_0, a_0) = \{1 + \exp[(r - r_0 A^{1/3})/a_0]\}^{-1}$$

and $V_C(r)$ is the Coulomb potential due to a charge distribution $f(r, r_C, a_C)$ with $r_C = (1.106 + 1.05 \times 10^{-4} A)$ F and $a_C = 0.502$ F.[3,4] In this form, the model has 10 adjustable parameters: V_{RS}, W_V, W_S, V_{so}, r_R, a_R, r_I, a_I, r_{so}, and a_{so}.

The data were analyzed in three ways: (1) using the cross-section and polarization data, (2) using only the polarization data, and (3) using only the cross-section data. For procedure (3), the spin-orbit parameters, V_{so}, r_{so}, and a_{so}, were fixed at the values obtained in procedure (2) because of the insensitivity of the fitting to these parameters when only cross-section data were used. Except for this restriction in procedure (3), the search routine varied all parameters simultaneously. The best-fit parameters obtained for ^{40}Ca, ^{56}Fe, and ^{59}Co are listed in Table II. The model predictions of procedure (1), together with the experimental points, are shown in Figs. 1 and 2.

TABLE II. Best-fit parameter sets obtained using the standard optical model for 30.3-MeV protons. Three combinations of experimental data were used: (1) elastic differential-cross-section data (of Ref. 7) and the present polarization data ($\sigma+P$); (2) elastic polarization data only (P) and; (3) elastic differential-cross-section data only (σ). In case (3), the spin-orbit parameters were fixed at the values found in case (2). Typical errors in $\langle r^2\rangle_{RS}^{1/2}$ and J_{RS}/A are ±0.15 F and ±15 MeV F^3.

Element	^{40}Ca			^{56}Fe			^{59}Co		
data analyzed	$\sigma+P$	P	σ	$\sigma+P$	P	σ	$\sigma+P$	P	σ
V_{RS} (MeV)	47.30	46.61	56.07	49.06	45.85	52.40	49.38	47.53	53.78
W_V (MeV)	0.09	0.02	4.50	3.13	0.82	2.38	2.88	1.76	1.74
W_S (MeV)	6.46	6.51	0.58	4.49	6.73	5.93	4.18	5.66	6.32
V_{so} (MeV)	4.48	4.41	4.41	6.60	6.27	6.27	6.54	5.78	5.78
r_R (F)	1.156	1.163	1.030	1.142	1.183	1.122	1.133	1.147	1.120
a_R (F)	0.739	0.740	0.861	0.742	0.706	0.733	0.759	0.742	0.726
r_I (F)	1.389	1.400	1.722	1.375	1.263	1.289	1.386	1.247	1.245
a_I (F)	0.568	0.539	0.193	0.593	0.713	0.615	0.651	0.862	0.670
r_{so} (F)	0.975	0.978	0.978	0.957	1.008	1.008	0.970	1.005	1.005
a_{so} (F)	0.480	0.464	0.464	0.672	0.640	0.640	0.636	0.548	0.548
$\langle r^2\rangle_{RS}^{1/2}$ (F)	4.11	4.13	4.20	4.37	4.38	4.30	4.43	4.42	4.33
J_{RS}/A (MeV F^3)	414	415	417	395	396	401	390	384	405
σ_R (mb)	926	900	881	1125	1175	1099	1193	1320	1134
σ_R(expt) (mb)	913±38[a]			1140±43[a]			1169±39[a]		
χ^2_σ	72.7	•••	27.3	19.5	•••	12.7	23.2	•••	9.4
χ^2_P	162.3	150.1	•••	30.1	24.0	•••	50.9	30.7	•••
χ^2_T	113.9	150.1	27.3	24.2	24.0	12.7	36.4	30.7	9.4

[a]Value at 28.5 MeV (see Ref. 8).

Figures 1 and 2 show that the data are being reasonably well represented by the model. However, examination of Table II shows that the A-dependent effects reported in Ref. 1 for ^{208}Pb, ^{120}Sn, and ^{58}Ni are continued for the present cases. Thus:
(a) The χ^2 values for ^{56}Fe and ^{59}Co are similar to those of ^{58}Ni and are appreciably greater for ^{40}Ca.
(b) The parameters obtained using the different combinations of data show significant variations which are greater the lower the A value.
(c) The spin-orbit radius parameters are significantly smaller than the real radius parameters and correspond to a peaking of the spin-orbit potential approximately 0.5 F inside the nucleon half-density point.

B. Folding-Model Analysis

The model of Greenlees, Pyle, and Tang[3,4] obtains the real parts of the potential by folding the nuclear proton $[\rho_p(r)]$ and neutron $[\rho_n(r)]$ density distributions with the appropriate components of the nucleon-nucleon potential. In previous work, which considered primarily cross-section data,[4] the quality of fit obtained was found to be relatively insensitive to the details of the nucleon-nucleon potential. These conclusions were not changed with the inclusion of more accurate polarization data in Ref. 1.[10] The nucleon-nucleon potential was therefore obtained from an analysis of low-energy nucleon-nucleon data, which considered both singlet and triplet interactions of different ranges, with a Gaussian form for each.[11]

The interaction potential used here may be written as

$$V(r) = V_C(r) + U_{RS} - iW_V f(r, r_I, a_I) + iW_S 4a_I \frac{d}{dr} f(r, r_I, a_I) + U_{so}, \quad (2)$$

where $V_C(r)$ is the Coulomb potential as used in Sec. III A, and

$$U_{RS} = -V_{RS} \frac{I_{nt} + \frac{1}{3}\alpha(I_{ns} + 2I_{ps})}{(I_{nt} + I_{pt}) + \alpha(I_{ns} + I_{ps})},$$

$$U_{so} = -V_{so} I_{so}(r) \vec{\sigma} \cdot \vec{l},$$

$$I_{ij}(r) = \int f_i(\vec{\eta}) g_j(|\vec{\eta} - \vec{r}|) d\vec{\eta},$$

$$\rho_i(r)/\rho_{i0} = f_i(r) = \{1 + \exp[(r - r_i A^{1/3})/a_i]\}^{-1},$$

$$g_j(r) = e^{-K_j r^2},$$

$i = p$ for proton, n for neutron,

$j = t$ for triplet, s for singlet,

$K_t = 0.415$ F^{-2},

$K_s = 0.292$ F^{-2},

$\alpha = V_{0s}/V_{0t} = 0.4341$.

The spin-orbit term I_{so} is obtained as described in Ref. 4 [Eq. (15)] using a Yukawa form for u_{ls} with a mean square radius of 0.5 F^2.

A phenomenological imaginary term is included in $V(r)$ to represent interactions other than elastic

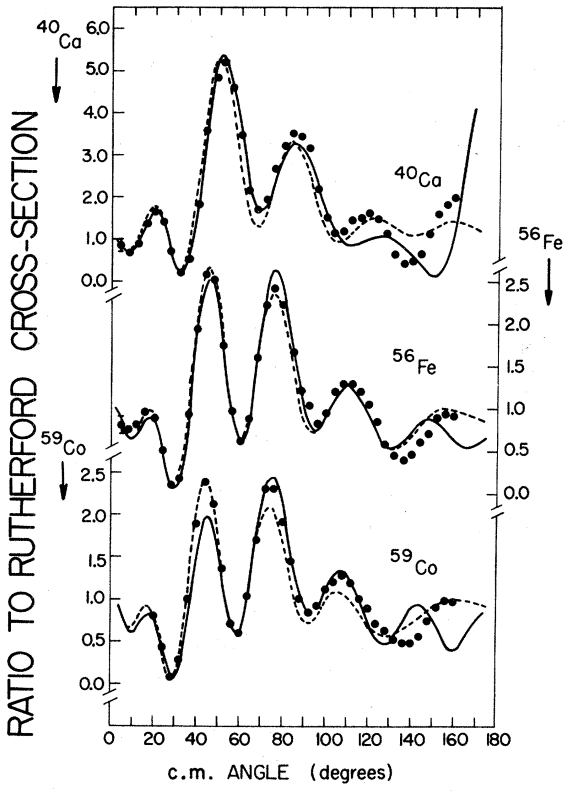

FIG. 1. Experimental differential-cross-section data points, with errors, for the elastic scattering of 30.3-MeV protons (Ref. 7), together with predictions obtained from analyzing cross-section and polarization data using: (1) standard optical model of Sec. III A (dashed line), and (2) folding model of Sec. III B (full line).

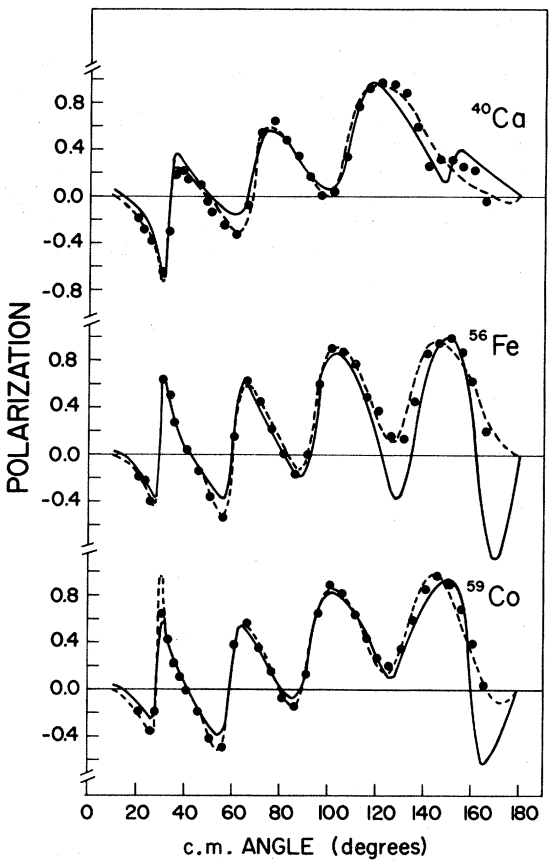

FIG. 2. Experimental polarization data points for the elastic scattering of 30.3-MeV polarized protons, together with predictions obtained from analyzing cross-section and polarization data using: (1) standard optical model of Sec. III A (dashed line), and (2) folding model of Sec. III B (full line). The error bars are less than the size of the points plotted.

scattering. This term has the same form as in Eq. (1).

The proton-distribution parameters are obtained from the measured charge distributions by unfolding the finite proton size giving: $r_p = (1.106 + 1.05 \times 10^{-4} A)$ F and $a_p = 0.454$ F.[3,4] This leaves eight adjustable parameters which are varied simultaneously to find a minimum in χ^2. The parameters are r_n, a_n, r_I, a_I, V_{RS}, V_{so}, W_V, and W_S, and the best-fit values obtained are listed in Table III. The corresponding model predictions are included in Figs. 1 and 2.

Table III indicates that for ^{56}Fe and ^{59}Co, and more so for ^{40}Ca, the representation of the data is less satisfactory with the folding model, the χ^2 values being 2 to 4 times greater, respectively, and the visual quality of the fits is noticeably worsened. This agrees with the trend found for ^{208}Pb, ^{120}Sn, and ^{58}Ni in Ref. 1 where it was attributed to the increased mathematical freedom present in the regular model because the spin-orbit and real geometries were independent.

The χ^2 values obtained with both models for the present data together with those reported earlier are listed in Table IV.

Tables II and III show that, as previously noted, the volume integral (J_{RS}) and the mean square radii ($\langle r^2 \rangle_{RS}$) of the real central potential (U_{RS}) are well defined and insensitive either to the detailed form of the potential used or to the type of data analyzed. Furthermore, the volume integral per nucleon (J_{RS}/A) is independent of A [and $(N-Z)/A$] to within the accuracy obtained. This latter result is in agreement with previous analyses of elastic proton data and has no obvious explanation. It is, however, consistent with the suggestion that the model is a good representation of the interaction for heavier (larger) nuclei but oversimplified for lighter (smaller) nuclei.

IV. CONCLUSIONS

An optical-model analysis has been presented of relatively accurate differential-cross-section and

TABLE III. Best-fit parameters using the singlet and triplet two-body potentials as outlined in the text. The present 30.3-MeV proton polarization data, together with the differential-cross-section data of Ref. 7 were analyzed simultaneously. The normalization of the spin-orbit term is different from that used in Table II. A strength here of about 2000 MeV corresponds to a strength of 6 MeV in Table II. Typical errors in $\langle r^2\rangle_n^{1/2}$, $\langle r^2\rangle_{RS}^{1/2}$, and J_{RS}/A are ±0.2 F, ±0.15 F, and ±15 MeV F^3. The experimental reaction cross sections quoted are from Ref. 8 for a proton energy of 28.5 MeV.

Element	^{40}Ca	^{56}Fe	^{59}Co
V_{RS} (MeV)	53.35	56.13	58.38
W_V (MeV)	0.85	4.97	6.28
W_S (MeV)	8.00	4.04	4.01
V_{so} (MeV)	1922	1649	1952
r_I (F)	1.267	1.388	1.349
a_I (F)	0.485	0.478	0.434
r_n (F)	1.288	1.138	1.126
a_n (F)	0.291	0.452	0.536
$\langle r^2\rangle_{RS}^{1/2}$ (F)	4.08	4.27	4.39
J_{RS}/A (MeV F^3)	425	396	416
σ_R (mb)	864	1091	1108
σ_R(expt) (mb)	913±38	1140±43	1169±39
χ^2_σ	69.0	29.5	62.7
χ^2_P	619.2	175.8	251.2
χ^2_T	321.8	94.5	152.9
$\langle r^2\rangle_n^{1/2}$ (F)	3.58	3.77	3.94
$\langle r^2\rangle_n^{1/2} - \langle r^2\rangle_p^{1/2}$ (F)	0.19	0.07	0.19

polarization data for the elastic scattering of 30.3-MeV protons from ^{40}Ca, ^{56}Fe, and ^{59}Co. Two forms of the model have been used, the standard ten-parameter form with independent geometries and the eight-parameter folding version of Greenlees, Pyle, and Tang[3,4] with the inclusion of singlet and triplet two-body forces.[1]

The formulation of the folding model used here is only strictly applicable to scattering by spin-zero nuclei. The data presented here for ^{59}Co are the first precision polarization data available for a non-spin-zero nucleus. It can be seen from Table IV that the quality of the folding-model fit is slightly worse for ^{59}Co than for the nearby nuclei ^{58}Ni and ^{56}Fe, which may result from the nuclear spin. However, the effect is rather small (less than 50% in χ^2), suggesting that the nuclear spin does not seriously complicate the description.

The results of the present analysis are entirely consistent with the conclusions of Ref. 1, which considered ^{58}Ni, ^{120}Sn, and ^{208}Pb. These features may be described as follows:

For medium-A nuclei, the standard optical model consistently achieves a better representation than the folding model. This is associated with the additional freedom in the spin-orbit radius parameter allowed in the standard version and produces a peaking of the spin-orbit interaction in a region of nearly constant nuclear density (about 0.5 F inside the half-density point for these nuclei).

TABLE IV. Compilation of best-fit χ^2 values obtained from Ref. 1 (^{58}Ni, ^{120}Sn, ^{208}Pb) and the present work (^{40}Ca, ^{56}Fe, ^{59}Co) using the standard 10-parameter model and the folding model to fit both cross-section and polarization data simultaneously.

Element	Standard model χ^2_σ	χ^2_P	χ^2_T	Folding model χ^2_σ	χ^2_P	χ^2_T
^{40}Ca	72.7	162.3	113.9	69.0	619.2	321.8
^{56}Fe	19.5	30.1	24.2	29.5	175.8	94.5
^{58}Ni	15.5	33.1	24.7	24.0	175.0	103.5
^{59}Co	23.2	50.9	36.4	62.7	251.2	152.9
^{120}Sn	8.1	13.5	10.7	11.7	40.8	25.5
^{208}Pb	3.8	11.4	7.8	3.8	17.2	10.9

The analysis also shows variations in parameters for medium-A nuclei dependent upon whether cross-section or polarization data, or both, are analyzed. The A-dependent variation in χ^2 values for the nuclei considered in this work and Ref. 1, both for the regular and folding models, indicates that either model is less satisfactory for lighter nuclei. (See Table IV.) However, it is not clear from the present work whether χ^2 gradually becomes worse as ^{40}Ca is approached or whether the χ^2 for ^{40}Ca is anomalously large as has been suggested by some workers.[3] More data of similar quality in the A = 40–50 region will be needed in order to determine which possibility is occuring.

These features, together with the absence of an isospin dependence of the real-central-potential volume integrals, and the inferior fit to inelastic data for medium-weight nuclei when the optical-model parameters involved have different real central and spin-orbit radius parameters[5,6] suggests that the optical-model description normally used for elastic scattering is less satisfactory for smaller systems where some second-order processes are playing a nonnegligible role. This could possibly be represented by an l dependence of the potential which would be expected to be most marked for low l values which in turn play a relatively more important role the smaller the nucleus.

Additional accurate and extensive data, together with an investigation of possible second-order processes, will be needed to test these suggestions.

ACKNOWLEDGMENTS

We would like to acknowledge the provision of experimental facilities by the Rutherford High Energy Laboratory, and the services of the University of Minnesota Numerical Analysis Center.

†Work supported in part by the U. S. Atomic Energy Commission, publication report No. COO-1265-101.

[1]G. W. Greenlees, V. Hnizdo, O. Karban, J. Lowe, and W. Makofske, Phys. Rev. C 2, 1063 (1970).

[2]F. D. Becchetti, Jr., and G. W. Greenlees, Phys. Rev. 182, 1190 (1969).

[3]G. W. Greenlees, G. J. Pyle, and Y. C. Tang, Phys. Rev. 171, 1115 (1968).

[4]G. W. Greenlees, W. Makofske, and G. J. Pyle, Phys. Rev. C 1, 1145 (1970).

[5]O. Karban, P. D. Greaves, V. Hnizdo, J. Lowe, and G. W. Greenlees, Nucl. Phys. A147, 461 (1970).

[6]V. Hnizdo, P. D. Greaves, O. Karban, and J. Lowe, in Proceedings of the Madison Conference on Polarization Phenomena in Nuclei, September, 1970 (to be published).

[7]B. W. Ridley and J. F. Turner, Nucl. Phys. 58, 497 (1964).

[8]J. F. Turner, B. W. Ridley, P. E. Cavanagh, G. A. Gard, and A. G. Hardacre, Nucl. Phys. 58, 509 (1964).

[9]G. J. Pyle, University of Minnesota, John H. Williams Laboratory of Nuclear Physics Report No. COO-1265-64 (unpublished).

[10]An improvement in χ^2 can be achieved for medium-weight elements if the nucleon-nucleon force parameters are allowed to depart from the "free" values in a manner which increases the surface isospin potential. This effect is most marked for ^{40}Ca where χ^2 is improved by a factor of 4 (V. Hnizdo, Ph.D. thesis, Birmingham University). This suggests a need for a surface-peaked real potential in these cases but it is not clear that such a peaking is in any way related to an isospin effect. It may, however, be a method of representing some of the effects neglected in the model.

[11]I. Reichstein and Y. C. Tang, Nucl. Phys. A139, 144 (1969).

PHYSICAL REVIEW C VOLUME 3, NUMBER 4 APRIL 1971

Measurement of Magnetic-Substate Populations Following the Reactions ^{16}O(^{7}Li, t)^{20}Ne and ^{16}O(^{6}Li, d)^{20}Ne†

D. P. Balamuth

Department of Physics, University of Pennsylvania, Philadelphia, Pennsylvania 19104

(Received 3 December 1970)

Particle-γ angular correlations using the reactions ^{16}O(^{7}Li, $t\gamma$)^{20}Ne and ^{16}O(^{6}Li, $d\gamma$)^{20}Ne have been measured. The populations of the various magnetic substates in the residual nucleus were extracted from the data. The results indicate the presence of other reaction mechanisms competing with direct transfer of an α particle.

I. INTRODUCTION

Attempts have been made to understand the structure of certain states in light nuclei by regarding them as made up of clusters of smaller composite groups for some time.[1,2] α particles form a natural unit for such a cluster; the tight binding of the α particle makes plausible the idea that α-like clusters can exist within a larger nucleus. It has also been pointed out that states with large α-cluster structure are often members of rotational bands.[3] Many resonant states have been observed with large α-particle widths, largely by measuring elastic scattering and reactions induced by α particles. Among the more interesting of these were the highly excited rotational states in ^{16}O, observed as resonances in the ^{12}C(α, α)^{12}C reaction by Carter, Mitchell, and Davis.[4]

More recently interest has centered on the study of α-particle structure in both bound and unbound states using nuclear reactions in which an α particle is transferred. There has been quite a bit of recent experimental work[5] involving the (^{7}Li, t) and (^{6}Li, d) reactions, among others. If such processes can be considered a direct reaction, i.e., one in which only a few nucleons participate, they can clearly be extremely useful in exploring the α-particle parentage of nuclear energy levels.

There are many problems involved in the analysis of the particle angular distributions using conventional distorted-wave theory. For example, in the ^{7}Li nucleus the α and triton clusters are in a relative p state, making the usual zero-range approximation impossible to apply. Nevertheless, in many cases the angular distributions do show the forward peaking expected qualitatively from a direct process[5]; furthermore, recent calculations using Coulomb-distorted plane-wave theory[6] have met with some success in predicting the observed behavior, especially the dependence of the cross section on excitation energy.

Because of the interest in this type of reaction it was considered desirable to investigate the reaction mechanism in more detail. The method of particle-γ angular correlations was chosen. In the present work the aim of the correlation measurements was not to elicit spectroscopic information, but rather to shed light on the mechanism